

Pleural Changes after Talc Pleurodesis in Patients with Underlying Malignancy: Comparison with Recurrent Malignant Pleural Lesions on CT and Fluorodeoxyglucose-Positron Emission Tomography/CT

악성 종양 환자에서 탈크 흉막 유착술 시행 후 나타난 흉막 변화: 재발된 악성 흉막 병변의 CT와 Fluorodeoxyglucose-Positron Emission Tomography/CT 소견과 비교

Beom Su Kim, MD, Hee Kang, MD, Jung Gu Park, MD

Department of Radiology, Kosin University Gospel Hospital, Busan, Korea

Purpose: To compare computed tomography (CT) and fluorodeoxyglucose-positron emission tomography/CT (FDG-PET/CT) findings of benign pleural changes with those of recurrent malignant pleural lesions in patients with a history of underlying malignancy after talc pleurodesis.

Materials and Methods: Of 194 patients who underwent talc pleurodesis, we retrospectively reviewed 16 patients for whom both follow-up CT and FDG-PET/CT were performed. The morphologic CT findings and maximum standard uptake values (SUV_{max}) were evaluated and compared between benign pleural changes and recurrent malignant pleural lesions.

Results: Twenty-two lesions were found in 16 patients; six patients had no evidence of active pleural disease (group 1) and 10 patients had recurrent malignant pleural lesions on radiological or clinical follow-up (group 2). Characteristic high-density pleural deposits [mean, 131 Hounsfield unit (HU); range, 28-251 HU] were seen along the pleural thickenings (mean, 13.4 mm; range, 4.9-62.3 mm) in 15 patients. The shape and thickness on CT and the SUV_{max} on FDG-PET/CT showed no significant differences between the two groups. On CT, the pre-contrast attenuation was higher in group 1 than group 2 (165 HU vs. 101 HU, respectively, $p = 0.030$), and the degree of enhancement was higher in group 2 than that in group 1 (29 HU vs. 48 HU, respectively, $p = 0.048$). Pleural effusions ($n = 5$) and other pleural thickening without high-density foci ($n = 4$) were observed only in group 2; however, no statistical significance was observed between the two groups.

Conclusion: Malignant pleural lesions can be characterized by lower pre-contrast attenuation and higher contrast enhancement, whereas benign pleural changes after talc pleurodesis are characterized by higher pre-contrast attenuation and lower contrast enhancement on CT.

Index terms

Talc Pleurodesis
Pleural Change
Talc Granuloma
CT
Positron Emission Tomography/CT

Received August 16, 2013; Accepted October 18, 2013

Corresponding author: Hee Kang, MD

Department of Radiology, Kosin University Gospel Hospital, 262 Gamcheon-ro, Seo-gu, Busan 602-702, Korea.

Tel. 82-51-990-6341 Fax. 82-51-255-2764

E-mail: soinvain@naver.com

This is an Open Access article distributed under the terms of the Creative Commons Attribution Non-Commercial License (<http://creativecommons.org/licenses/by-nc/3.0>) which permits unrestricted non-commercial use, distribution, and reproduction in any medium, provided the original work is properly cited.

INTRODUCTION

Pleurodesis is defined as the formation of a symphysis between the visceral and parietal pleura that prevents accumulation of air or liquid in the pleural space (1). Pleurodesis is performed by introducing sclerosing agents into the pleural cavity

or by surgical abrasion of the pleura (2). Although a number of other sclerosing agents have been used for pleurodesis, talc is considered the best sclerosant based on success rates (3, 4). Talc induces an intrapleural inflammatory response and plural fibrosis that obliterate the pleural space (2).

Pleural changes after talc pleurodesis include pleural thicken-

ing, nodularity, formation of pleural masses, and residual effusion (5, 6). Focal areas of high attenuation within the pleural changes representing talc deposition and dystrophic calcification can be seen on computed tomography (CT) (2, 5, 7). Recent reports have documented talc-related fluorodeoxyglucose (FDG) uptake within high-attenuation areas (8-16). Pleural changes after talc pleurodesis make it difficult to distinguish between benign inflammatory processes and malignant pleural lesions, particularly in patients with a history of underlying malignancy.

The purpose of this study was to characterize the CT and FDG-positron emission tomography (PET)/CT findings of benign pleural changes and compare them to those of recurrent malignant pleural lesions after talc pleurodesis in patients with a history of underlying malignancy.

MATERIALS AND METHODS

Patients

From January 2004 to December 2011, 194 patients who had undergone talc pleurodesis at our institution were retrospectively reviewed. Of these, we enrolled 16 patients who had a history of malignancy and who underwent follow-up CT and FDG-PET/CT scans. The mean age of the study group was 54 years (range, 41-76 years). Eleven patients were male and five were female. The underlying malignancies were lung cancer ($n = 13$), malignant mesothelioma ($n = 1$), esophageal cancer ($n = 1$), and cervical cancer ($n = 1$). Patient characteristics are listed in Table 1. Six patients had no evidence of active pleural disease (group 1) and 10 patients had recurrent malignant pleural lesions (group 2). Group 1 was pathologically confirmed by percutaneous needle biopsy (two patients) or clinically regarded as having benign conditions. Group 1 did not show evidence of recurrent

pleural lesion based on imaging studies and clinical follow-up of at least 6 months. The mean follow-up period for group 1 was 16 months (range, 6-23 months). Group 2 was confirmed to have recurrent malignant pleural lesions such as pleural or mediastinal invasion and metastasis based on clinical presentation and follow-up studies. The mean follow-up period of group 2 was 9 months (range, 4-16 months). Our institutional review board approved this retrospective study and did not require informed patient consent.

CT Scans

CT scans were acquired by a helical technique using a Somatom Plus-4 (Siemens Medical Solutions, Erlangen, Germany) or a Somatom Sensation 64 (Siemens Medical Solutions) scanners. Scanning was performed from the lower part of the neck to the middle portion of the kidneys. All scanning was performed after intravenous (IV) administration of contrast medium (140 mL Iopamidol, Pamiray 300, Dongkuk Pharm., Seoul, Korea) with a power injector (Mallinckrodt, Tyco and Vistron CT, Medrad, Arrendale, PA, USA) at an injection rate of 2.5 mL/sec. The scanning parameters were 120 kVp; 90 and 150 mA; beam width, 2.5 mm; and table speed, 15 mm per rotation. Data were interfaced directly to a picture-archiving and communicating system (PACS; Marosis m-view, Infinitt, Korea), which displayed all image data on two monitors (1536 × 2048 image matrices, 8-bit viewable gray scale, and 60-foot-lambert luminescence). Scans were viewed with both mediastinal (window width, 400 H; window level, 20 H) and lung (window width, 1500 H; window level, -700 H) window settings.

PET/CT Scanning

All patients fasted for at least 6 hours and had a serum glucose level < 140 mg/dL before the IV injection of FDG. Scans were acquired for 60 minutes after administration using a PET/CT system (CTI, Knoxville, TN, USA) consisting of a full-ring PET scanner and a dual-detector-row spiral CT scanner (Somatom Emotion duo, Biograph, Erlangen, Germany). CT scans were performed from the head to the pelvic floor according to a standard protocol with the following settings: 130 kVp; 30 mA; tube rotation time, 0.8 seconds per rotation; pitch, 6; and section thickness, 5 mm to match the PET section thickness. Immediately after non-enhanced CT, PET was performed in the identical

Table 1. Patient Characteristics and Types of Malignancy

Patient characteristics ($n = 16$)	
Male/Female	11/5
Mean age (range)	54 (41-76)
Types of malignancies	
Lung cancer	13
Adenocarcinoma	7
Squamous cell lung cancer	6
Malignant mesothelioma	1
Esophageal cancer	1
Cervical cancer	1



Fig. 1. A 49-year-old woman who underwent a right lower lobectomy due to lung adenocarcinoma (group 1).

A. Pre-contrast CT scan taken 14 months after talc pleurodesis shows nodular pleural thickening with a focal area of high attenuation in the right upper thorax (arrow).

B. Contrast-enhanced CT scan shows contrast enhancement (arrow).

C. FDG-PET/CT scan shows intense FDG uptake (arrow).

Note.—FDG-PET/CT = fluorodeoxyglucose-positron emission tomography/CT

transverse field of view. PET datasets were obtained via iterative reconstruction with an ordered subset expectation maximization algorithm and by the application of segmented attenuation correction (two iterations, 28 subsets) to CT data. Co-registered scans were displayed using software that enabled image fusion and analysis.

Imaging Analysis

Imaging analyses were performed using morphologic CT findings including shape (nodular, linear, and patchy), thickness (mm), average attenuation [Hounsfield unit (HU)], and degree of enhancement (HU) of the pleural lesions. Attenuation (HU) was measured using the elliptical region of interest (ROI) around high-density pleural lesions, and the degrees of enhancement were recorded as the difference in attenuation between enhanced and non-enhanced images. The highest metabolic activity was evaluated using measurements of maximum standard uptake values (SUV_{max}) within the same ROI used for the average attenuation measurements. When a patient had two or more discontinuous lesions, images were separately evaluated for each lesion. All measured values were compared between groups 1 and 2.

Statistical Analysis

Differences in lesion shape and additional findings between groups 1 and 2 were assessed using Fisher's exact test. The Mann-Whitney U-test was used to compare thickness, attenuation, degree of enhancement, and SUV_{max} . p -values < 0.05 were considered significant. Statistical analysis was performed using PASW statistics 20 (SPSS Inc., Chicago, IL, USA).

Table 2. Shapes of Pleural Lesions on CT

	Group 1	Group 2	Total
Nodular	2	1	3
Linear	5	5	10
Patchy	3	6	9
Total	10	12	22

Note.—Data are number of pleural lesions.

RESULTS

Characteristic high-density pleural deposits with contrast enhancement on CT and increased uptake on FDG-PET/CT were seen along the pleural thickening in 15 patients (Fig. 1). The total number of pleural lesions was 22, and the mean number of pleural lesions per patient was 1.4 (range, 1-3). Five patients had two or more discontinuous lesions (Fig. 2).

Shape

Of 22 pleural lesions, there were nodular patterns in three lesions (group 1, $n = 2$; group 2, $n = 1$), linear patterns in 10 (group 1, $n = 5$; group 2, $n = 5$), and patchy distributions in nine (group 1, $n = 3$; group 2, $n = 6$) (Figs. 2, 3). The shapes of the pleural lesions are summarized in Table 2. No significant differences were observed in lesion shape between groups 1 and 2 ($p = 0.607$).

Pleural Thickening

The thicknesses of the pleural lesions varied widely on CT (mean, 13.4 mm; range, 4.9-62.3 mm). The mean thicknesses of the pleural lesions were 11.7 mm (range, 7.0-16.9 mm) and 14.8 mm (range, 4.9-62.3 mm) in groups 1 and 2, respectively. No significant differences were observed in pleural thickening be-

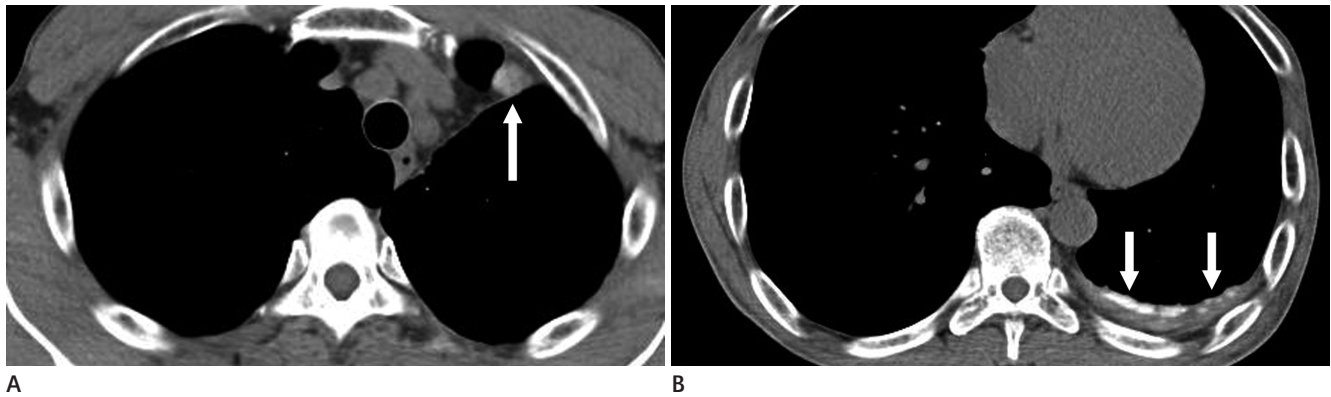


Fig. 2. A 53-year-old man who underwent a left lower lobectomy due to lung adenocarcinoma (group 1).

A. Pre-contrast CT scan taken 20 months after talc pleurodesis shows a focal area of high attenuation with nodular pleural thickening in the left upper anterior thorax (arrow).

B. Diffuse pleural thickening with a linear high attenuation area was seen in the left lower posterior thorax (arrows).



Fig. 3. A 65-year-old man who underwent right upper wedge resection due to squamous cell lung cancer (group 2).

A, B. Pre-contrast (**A**) and contrast-enhanced (**B**) CT scans taken 3 months after talc pleurodesis show a high-density pleural thickening with patchy distribution and contrast enhancement in the right upper hemithorax (arrow).

C. Contrast-enhanced CT scans taken 10 months after talc pleurodesis show a recurrent mass with pleural involvement in the right upper hemithorax.

tween the groups ($p = 0.356$).

Attenuation and Enhancement

The majority of pleural abnormalities were associated with areas of high attenuation (mean, 131 HU; range, 28-251 HU). The mean attenuations of the pleural lesions were 166 HU (range, 65-251 HU) in group 1 and 101 HU (range, 28-218 HU) in group 2. Attenuation of pleural lesions was significantly higher in group 1 than that in group 2 ($p = 0.030$). After contrast administration, all pleural lesions except two showed increased attenuation of 20 HU or more. One of the two unusual lesions belonged to group 1, and the other belonged to group 2. The mean degree of enhancement for all lesions was 40 HU (range, 5-73 HU). Although most pleural lesions showed contrast enhancement, the degree of enhancement was significantly higher in group 2 than that in group 1 ($p = 0.048$) (Fig. 3). The mean degree of enhancement was 29 HU (range, 5-62 HU) and 48 HU (range, 12-73 HU) in group 1 and group 2, re-

spectively.

Maximum Standard Uptake Value

The areas of SUV_{max} corresponded to high attenuation pleural abnormalities in all lesions (mean, 12.04; range, 4.34-42.65). The mean SUV_{max} of pleural lesions was 10.89 (range, 7.74-18.25) and 12.99 (range, 4.34-42.65) in groups 1 and 2, respectively. No significant differences were observed between the groups ($p = 0.598$). Values for pleural thickening, attenuation, degree of enhancement and SUV_{max} are summarized in Table 3.

Additional Findings

Pleural effusions ($n = 5$) and other pleural thickenings without high-density foci ($n = 4$) were seen only in group 2 (Fig. 4). However, the frequencies of pleural effusion and other pleural thickening were not significantly higher in group 2 than those in group 1 (pleural effusion, $p = 0.093$; other pleural thickening, $p = 0.234$) (Table 3).

Table 3. Differences in Pleural Lesions and Additional Findings between Group 1 and Group 2

	Thickness (mm)*	Attenuation (HU)*	Degree of Enhancement (HU)*	SUV _{max} *	Pleural Effusion [†]	Other Pleural Thickening [†]
Group 1	11.67 ± 3.44	165.80 ± 52.36	29.13 ± 17.18	10.89 ± 3.54	0/6	0/6
Group 2	14.79 ± 15.98	101.16 ± 65.00	48.18 ± 19.65	12.99 ± 12.07	5/10	4/10
<i>p</i> -value	0.356	0.030	0.048	0.598	0.093	0.234

Note. — *p*-value < 0.05 is statistically significant.

*Calculated by Mann-Whitney U tests. Data are mean ± standard deviation.

[†]Calculated by Fisher's exact tests. Data are number of patients.

HU = Hounsfield units, SUV_{max} = maximum standard uptake value

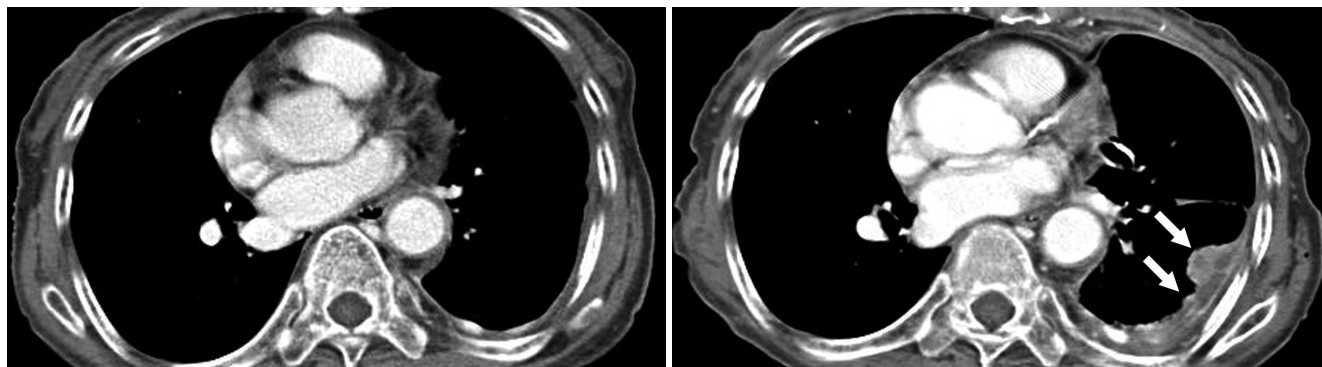


Fig. 4. A 77-year-old woman with malignant mesothelioma (group 2).
A. Contrast-enhanced CT scan taken 3 months after talc pleurodesis shows an area of high density with pleural thickening in the left hemithorax.

B. Eighteen months later, enhancing pleural thickening and nodules arose from the previously noted high-density pleural lesion (arrows).

DISCUSSION

Bethune (17) previously described anatomic changes in the pleura following talc pleurodesis in animal studies and observed that despite uniform scattering of talc powder over the pleura during thoracotomy, the powder subsequently accumulated into well-demarcated nodules. Jones (18) also described the presence of talc granulomata and pleural fibrosis after talc pleurodesis. Granulomatous giant cell reactions surrounding talc crystals in the pleura have been described in recent studies (6, 19).

The CT appearance of pleural changes after talc pleurodesis has not been widely reported. Murray et al. (5) observed typical findings after talc administration that presented as variable degrees of pleural thickening and nodularity with focal high attenuation areas. Narayanaswamy et al. (2) also described the presence of high-density deposits after talc pleurodesis. Various shapes and locations of lesions may occur because the appearance of talc-related pleural lesions is greatly influenced by the method of talc administration and the position of the patient (5). Most deposits have been described as linear or nodular pleural lesions (2, 5). Similar morphological findings were also ob-

served in our study. Among the diverse shapes of deposits, a patchy and linear pattern was much more frequently observed than a nodular pattern. However, no differences were observed between benign and malignant samples.

There is controversy regarding the degree of contrast enhancement in talc-related pleural lesions. Kwek et al. (10) described seven patients who underwent CT scans with and without IV contrast and found no evidence of increased enhancement in areas of pleural thickening after contrast administration. In contrast, Avila et al. (7) observed contrast enhancement in stable pleural lesions after talc pleurodesis and proposed that fibrotic tissue within the pleural lesion may variably enhance depending on the amount of vascular granulation tissue. In our study, all pleural lesions except two showed increases in attenuation of 20 HU or more after contrast enhancement. Moreover, the degree of enhancement was significantly higher in recurrent malignant lesions than benign pleural changes.

The SUV_{max} of pleural lesions was not significantly different between the two groups. According to previous studies, pleural macrophages are activated during the inflammatory process after talc pleurodesis and are the most likely cause of pleural FDG up-

take (11). Increased FDG uptake is persistent after talc pleurodesis, which indicates chronic influx and efflux of inflammatory cells (14). The stability of talc lesions on PET and PET/CT scan has been observed in case reports of patients followed for up to 42 years after talc pleurodesis (8-12, 15, 16, 20).

CT appearance after talc pleurodesis may simulate other conditions such as recurrence or metastasis, particularly in patients with a history of malignancy. Characteristic pleural thickening with high attenuation and a history of pleurodesis helps clinicians differentiate talc deposits from diverse pleural abnormalities (2). The use of FDG-PET/CT to distinguish malignant pleural involvement from benign inflammatory processes after talc pleurodesis remains challenging. Pleural lesions with increased FDG uptake that correspond to high attenuation on CT in patients with a history of talc pleurodesis is a typical finding of reactive inflammation (21). In contrast, pleural lesions without high-density foci associated with FDG uptake in follow-up studies should raise suspicion for malignant lesions.

In our study, pleural effusions and other pleural thickenings without high-density foci were seen only in the recurrent malignant group. Although the frequencies were not statistically significant between the two groups, we believe that these additional findings can be used to distinguish recurrent malignant lesions from benign pleural changes after talc pleurodesis.

Our study had limitations. First, it was a retrospective analysis of a small patient sample. Second, only two patients had histologically proven diagnoses by percutaneous biopsy. In the remaining patients, the lesions were assumed to be benign or malignant on the basis of follow-up imaging and clinical findings. Although not ideal, this is a recognized method for assessing pleural recurrence or metastasis. Third, we regarded the tumors as benign or malignant without confirming each lesion in patients with multiple lesions, which is a considerable weakness because benign and malignant lesions may exist concurrently in one patient.

In conclusion, pleural changes after talc pleurodesis are revealed as high-density pleural thickening with increased FDG uptake in both benign inflammatory processes and malignant lesions in patients with a history of malignancy. Malignant pleural lesions were characterized by lower pre-contrast attenuation and higher contrast enhancement, whereas benign pleural changes after talc pleurodesis were characterized by higher pre-

contrast attenuation and lower contrast enhancement on CT. Our findings may help clinicians distinguish recurrent malignant pleural lesions from benign inflammatory processes after talc pleurodesis in patients with a history of malignancy.

REFERENCES

- Rodriguez-Panadero F, Montes-Worboys A. Mechanisms of pleurodesis. *Respiration* 2012;83:91-98
- Narayanaswamy S, Kamath S, Williams M. CT appearances of talc pleurodesis. *Clin Radiol* 2007;62:233-237
- Shaw P, Agarwal R. Pleurodesis for malignant pleural effusions. *Cochrane Database Syst Rev* 2004;CD002916
- Tan C, Sedrakyan A, Browne J, Swift S, Treasure T. The evidence on the effectiveness of management for malignant pleural effusion: a systematic review. *Eur J Cardiothorac Surg* 2006;29:829-838
- Murray JG, Patz EF Jr, Erasmus JJ, Gilkeson RC. CT appearance of the pleural space after talc pleurodesis. *AJR Am J Roentgenol* 1997;169:89-91
- Williams T, Gostelow B, Woods D, Spyt T. Apical pleural mass developing following talc pleurodesis. *Respir Med* 1998;92:358-359
- Avila NA, Dwyer AJ, Rabel A, DeCastro RM, Moss J. CT of pleural abnormalities in lymphangioleiomyomatosis and comparison of pleural findings after different types of pleurodesis. *AJR Am J Roentgenol* 2006;186:1007-1012
- Murray JG, Erasmus JJ, Bahtiarian EA, Goodman PC. Talc pleurodesis simulating pleural metastases on 18F-fluorodeoxyglucose positron emission tomography. *AJR Am J Roentgenol* 1997;168:359-360
- Weiss N, Solomon SB. Talc pleurodesis mimics pleural metastases: differentiation with positron emission tomography/computed tomography. *Clin Nucl Med* 2003;28:811-814
- Kwek BH, Aquino SL, Fischman AJ. Fluorodeoxyglucose positron emission tomography and CT after talc pleurodesis. *Chest* 2004;125:2356-2360
- Nguyen M, Varma V, Perez R, Schuster DM. CT with histopathologic correlation of FDG uptake in a patient with pulmonary granuloma and pleural plaque caused by remote talc pleurodesis. *AJR Am J Roentgenol* 2004;182:92-94
- Ahmadzadehfar H, Palmedo H, Strunk H, Biersack HJ, Habibi

- E, Ezziddin S. False positive 18F-FDG-PET/CT in a patient after talc pleurodesis. *Lung Cancer* 2007;58:418-421
13. Al-Sarraf N, Doddakula K, Wedde T, Young V. Positron emission tomography staging of pleural deposits following Monaldi's procedure: an accurate reflection or a false staging? *Interact Cardiovasc Thorac Surg* 2007;6:260-261
 14. Nguyen NC, Tran I, Hueser CN, Oliver D, Farghaly HR, Osman MM. F-18 FDG PET/CT characterization of talc pleurodesis-induced pleural changes over time: a retrospective study. *Clin Nucl Med* 2009;34:886-890
 15. Peek H, van der Bruggen W, Limonard G. Pleural FDG Uptake More Than a Decade after Talc Pleurodesis. *Case Rep Med* 2009;2009:650864
 16. Tenconi S, Luzzi L, Paladini P, Voltolini L, Gallazzi MS, Granato F, et al. Pleural granuloma mimicking malignancy 42 years after slurry talc injection for primary spontaneous pneumothorax. *Eur Surg Res* 2010;44:201-203
 17. Bethune N. Pleural poudrage. A new technique for the deliberate production of pleural adhesions as a preliminary to lobectomy. *J Thorac Surg* 1935;4:251-261
 18. Jones GR. Treatment of recurrent malignant pleural effusion by iodized talc pleurodesis. *Thorax* 1969;24:69-73
 19. Ahmed Z, Shrager JB. Mediastinal talcoma masquerading as thymoma. *Ann Thorac Surg* 2003;75:568-569
 20. De Weerd S, Noppen M, Everaert H, Vincken W. Positron emission tomography scintigraphy after thoracoscopic talcage. *Respiration* 2004;71:284
 21. Leung AN, Müller NL, Miller RR. CT in differential diagnosis of diffuse pleural disease. *AJR Am J Roentgenol* 1990;154:487-492

악성 종양 환자에서 탈크 흉막 유착술 시행 후 나타난 흉막 변화: 재발된 악성 흉막 병변의 CT와 Fluorodeoxyglucose-Positron Emission Tomography/CT 소견과 비교

김범수 · 강 희 · 박정구

목적: 악성 종양의 기왕력이 있는 환자에서 탈크 흉막 유착술 이후에 발생한 양성 흉막 변화와 재발성 악성 흉막 질환의 CT와 fluorodeoxyglucose-positron emission tomography (이하 FDG-PET)/CT 소견을 비교해 보고자 한다.

대상과 방법: 탈크 흉막 유착술을 시행한 194명의 환자 중, 시술 후 추적 CT와 FDG-PET/CT 촬영을 시행한 16명의 환자를 대상으로 하였다. 흉막 병변의 CT와 FDG-PET/CT 소견을 평가하고 양성 흉막 변화와 재발성 악성 흉막 병변의 소견을 비교하였다.

결과: 악성 종양의 기왕력이 있는 16명의 환자에서 22개의 흉막 병변이 탈크 흉막 유착술 이후에 발생하였다. 추적관찰에서 양성 흉막 변화가 6명(집단 1)이었으며 재발성 악성 흉막 병변이 10명(집단 2)이었다. 특징적인 고음영[mean, 131 Hounsfield unit (이하 HU); range, 28~251 HU] 동반한 흉막 비후가(mean, 13.4 mm; range, 4.9~62.3 mm) 15명의 환자에서 나타났다. CT에서 보인 모양, 두께와 FDG-PET/CT에서 측정된 maximum standard uptake values는 두 집단 간에 유의한 차이가 없었다. CT에서 조영증강 전 감쇠값은 집단 1에서 더 높게 나타났으며(165 HU vs. 101 HU, $p = 0.030$), 조영증강의 정도는 집단 2에서 더 높게 측정되었다(29 HU vs. 48 HU, $p = 0.048$). 집단 2에서만 흉막 삼출($n = 5$)과 고음영의 침착이 동반되지 않은 흉막비후($n = 4$)가 관찰되었지만 두 집단 간에 통계적 유의성은 없었다.

결론: 탈크 흉막 유착술 이후에 발생한 양성 흉막 변화와 비교했을 때, 악성 흉막 병변은 조영증강 전 CT에서 더 낮은 감쇠값을 보이는 데 비해 조영증강 후 CT에서 더 높은 조영증강 소견을 보인다.

고신대학교 복음병원 영상의학과